

# Vibrations of bridges with continuous main girders

Autor(en): **Koloušek, Vladimir**

Objektyp: **Article**

Zeitschrift: **IABSE publications = Mémoires AIPC = IVBH Abhandlungen**

Band (Jahr): **19 (1959)**

PDF erstellt am: **24.09.2024**

Persistenter Link: <https://doi.org/10.5169/seals-16952>

## **Nutzungsbedingungen**

Die ETH-Bibliothek ist Anbieterin der digitalisierten Zeitschriften. Sie besitzt keine Urheberrechte an den Inhalten der Zeitschriften. Die Rechte liegen in der Regel bei den Herausgebern.

Die auf der Plattform e-periodica veröffentlichten Dokumente stehen für nicht-kommerzielle Zwecke in Lehre und Forschung sowie für die private Nutzung frei zur Verfügung. Einzelne Dateien oder Ausdrucke aus diesem Angebot können zusammen mit diesen Nutzungsbedingungen und den korrekten Herkunftsbezeichnungen weitergegeben werden.

Das Veröffentlichen von Bildern in Print- und Online-Publikationen ist nur mit vorheriger Genehmigung der Rechteinhaber erlaubt. Die systematische Speicherung von Teilen des elektronischen Angebots auf anderen Servern bedarf ebenfalls des schriftlichen Einverständnisses der Rechteinhaber.

## **Haftungsausschluss**

Alle Angaben erfolgen ohne Gewähr für Vollständigkeit oder Richtigkeit. Es wird keine Haftung übernommen für Schäden durch die Verwendung von Informationen aus diesem Online-Angebot oder durch das Fehlen von Informationen. Dies gilt auch für Inhalte Dritter, die über dieses Angebot zugänglich sind.

# **Vibrations of Bridges with Continuous Main Girders**

*Vibrations dans les ponts à poutres principales continues*

*Schwingungen der Brücken mit durchlaufenden Hauptträgern*

VLADIMÍR KOLOUŠEK

Prof. Ing. Dr., Praha

## **Introduction**

The problem of forced vibrations of continuous beams acted upon by moving loads which produce harmonically alternating vertical forces had been studied by the author of this paper some years ago<sup>1)</sup>. At that time the author theoretically analysed and numerically calculated the time-variation of the deflection of the centre of the middle span of a three-span beam, on the assumption that a two-cylinder, 100-ton locomotive is crossing the structure, and that the driving axles of the engine produce centrifugal forces  $P$  equal to  $0.6N^2$  ( $P$  in tons [metric], if  $N$  denotes number of revolutions per second).

It was, however, not possible at that time to check the calculated values experimentally and only a few years later dynamical measurements on an actual structure were made possible.

The spans, weight and stiffness of this actual structure as well as the dynamical effects of the locomotive used for the load test were different from those on which the above mentioned theoretical analysis had been based. The numerical example presented in this paper is worked out with assumptions which correspond to the actual structure and engine used at the mentioned load test.

---

<sup>1)</sup> KOLOUŠEK, "Stavebná dynamika spojitých nosníků a rámových soustav". Prague 1950. German translation "Baudynamik der Durchlaufträger und Rahmen". Leipzig 1953. Fachbuchverlag. French translation "Calcul des efforts dynamiques dans les ossatures rigides". Paris, Dunod, 1959.

### I. Brief review of the theoretical analysis

#### a) Free vibrations

The natural frequencies and modes of free vibrations of continuous beams with mass and cross section uniform along the individual spans can be analysed by the slope-deflection method. From the equilibrium of moments at any isolated joint  $K$  we have for free oscillations

$$M_{K,K-1} + M_{K,K+1} = 0, \quad (1)$$

where  $M_{K,K-1}$ ,  $M_{K,K+1}$  are end-moments of the bars  $K, K-1$  and  $K, K+1$  respectively.

For the case that the respective bar is continuous on both sides we have

$$M_{K,K-1} = \frac{E J_{K,K-1}}{l_{K,K-1}} [F_2(\lambda_{K,K-1}) \gamma_K + F_1(\lambda_{K,K-1}) \gamma_{K-1}], \quad (2)$$

where the notation is as follows:

$E$  modulus of elasticity,

$J$  moment of inertia of cross-section,

$l$  length of span,

$$\lambda = l \sqrt[4]{\frac{\mu \omega^2}{E J}},$$

$$F_1(\lambda) = -\lambda \frac{\sinh \lambda - \sin \lambda}{\cosh \lambda \cos \lambda - 1},$$

$$F_2(\lambda) = -\lambda \frac{\cosh \lambda \sin \lambda - \sinh \lambda \cos \lambda}{\cosh \lambda \cos \lambda - 1},$$

$\gamma_K$  angle of rotation of the joint  $K$ .

If the respective span has a hinge at the joint  $K$  we have

$$M_{K,K-1} = \frac{E J_{K,K-1}}{l_{K,K-1}} F_7(\lambda_{K,K-1}) \gamma_K, \quad (3)$$

where

$$F_7(\lambda) = \lambda \frac{2 \sinh \lambda \sin \lambda}{\cosh \lambda \sin \lambda - \sinh \lambda \cos \lambda}. \quad ^2)$$

If we write down eq. (1) for all the joints of a given system, we obtain a set of simultaneous homogenous linear equations. By setting the determinant of this set equal to zero we obtain the "frequency equation" for calculating the natural angular frequencies  $\omega_{(1)}$ ,  $\omega_{(2)}$ ,  $\omega_{(3)}$  etc. of the system. From the ratios of the subdeterminants we may then calculate the ratios of the rotations of joints  $\frac{\gamma_{K+1}}{\gamma_K}$ , which already determine the shape of the individual natural modes of vibration.

<sup>2)</sup> Tables of  $F(\lambda)$ -functions are given in 1).

The  $k$ -th natural mode is given by the formula

$$v_{(k)}(x) = C_1 \cosh \lambda \frac{x}{l} + C_2 \sinh \lambda \frac{x}{l} + C_3 \cos \lambda \frac{x}{l} + C_4 \sin \lambda \frac{x}{l}, \quad (4)$$

where  $v_{(k)}(x)$  denotes the vertical deflection in any point  $x$  for the  $k$ -th natural mode and

$$\lambda = l \sqrt[4]{\frac{\mu \omega_{(k)}^2}{EJ}}. \quad (5)$$

The constants of integration  $C$  are determined from the conditions at the ends of the bar.

If the span  $K-1, K$  is continuous at both ends we have

$$C_1 = -C_3 = -\frac{l}{2\lambda^2} [F_2(\lambda) \gamma_{K-1} + F_1(\lambda) \gamma_K], \quad (6)$$

$$C_2 = \frac{l}{2\lambda^3} [-F_4(\lambda) \gamma_{K-1} + F_3(\lambda) \gamma_K] + \frac{l}{2\lambda} \gamma_{K-1}, \quad (7)$$

$$C_4 = -C_2 + \frac{l}{\lambda} \gamma_{K-1}, \quad (8)$$

where

$$F_3(\lambda) = -\lambda^2 \frac{\cosh \lambda - \cos \lambda}{\cosh \lambda \cos \lambda - 1},$$

$$F_4(\lambda) = \lambda^2 \frac{\sinh \lambda \sin \lambda}{\cosh \lambda \cos \lambda - 1}.$$

The formulæ (6), (7), and (8) we obtain from eq. (4) considering the conditions at the ends, viz.

$$v_{(k)}(0) = v_{(k)}(l) = 0, \quad \frac{dv_{(k)}(0)}{dx} = \gamma_{K-1}, \quad \frac{dv_{(k)}(l)}{dx} = \gamma_K.$$

If the bar  $K, K-1$  is hinged at the point  $K-1$ , the conditions at the ends of the bar become

$$v_{(k)}(0) = v_{(k)}(l) = 0, \quad \frac{d^2 v_{(k)}(0)}{dx^2} = 0, \quad \frac{dv_{(k)}(l)}{dx} = \gamma_K$$

and we obtain for the constants of integration

$$C_1 = C_3 = 0, \quad (9)$$

$$C_2 = \frac{l}{\lambda} \frac{\sin \lambda}{\cosh \lambda \sin \lambda - \sinh \lambda \cos \lambda} \gamma_K, \quad (10)$$

$$C_4 = -\frac{l}{\lambda} \frac{\sinh \lambda}{\cosh \lambda \sin \lambda - \sinh \lambda \cos \lambda} \gamma_K. \quad (11)$$

If the bar  $K-1, K$  is hinged at the point  $K$  the end-conditions are

$$v_{(k)}(0) = v_{(k)}(l) = 0, \quad \frac{dv_{(k)}(0)}{dx} = \gamma_{K-1}, \quad \frac{d^2 v_{(k)}(l)}{dx^2} = 0$$

and we have 
$$C_1 = -C_3 = -\frac{l}{2\lambda^2} F_7(\lambda) \gamma_{K-1}, \quad (12)$$

$$C_2 = -\left(\frac{l}{2\lambda^3} F_9(\lambda) - \frac{l}{2\lambda}\right) \gamma_{K-1}, \quad (13)$$

$$C_4 = -C_2 - \frac{l}{\lambda} \gamma_{K-1}, \quad (14)$$

where 
$$F_9(\lambda) = -\lambda^2 \frac{\cosh \lambda \sin \lambda + \sinh \lambda \cos \lambda}{\cosh \lambda \sin \lambda - \sinh \lambda \cos \lambda}.$$

*b) Forced vibrations*

If the span of the bridge is large and the magnitude of the moving load is constant, then the dynamical effects produced are small, and the deflections may be calculated in the same way as for statical load only.

If an harmonically alternating force  $P \sin \Omega t$  moves along the bridge at constant speed  $c$ , forced vibrations of the structure are excited, and in this case the dynamical effects may be investigated by resolving the vibration into a series of natural modes<sup>3)</sup>. The differential equation for the vertical vibrations in this case becomes

$$\mu \frac{\partial^2 v(x, t)}{\partial t^2} + 2\mu \omega_b \frac{\partial v(x, t)}{\partial t} + EJ \frac{\partial^4 v(x, t)}{\partial x^4} = p(x, t), \quad (15)$$

where the notations are as follows:

- $\mu$  is the uniformly distributed mass per unit of length.
- $x$  is the abscissa of the point in question if the origin is at the left end of each span.
- $t$  is the time in seconds.
- $v(x, t)$  is the vertical deflection of the point  $x$  at the time  $t$ .
- $\omega_b$  is the damping factor (dimension the same as frequency).
- $p(x, t)$  is the load per unit length variable with  $x$  and  $t$ . If the bar is loaded only by an alternating force  $P \sin \Omega t$  at the point  $x = a = ct$ , it follows that  $p(x, t)$  is equal to zero at all points with the exception of the point  $x = a = ct$ .
- $P$  is the amplitude of the harmonically alternating force.
- $\Omega = 2\pi N$  is the angular frequency of  $P$ .
- $N$  is the frequency of  $P$ , in practice it is the number of revolutions p. sec. of the driving axles.

We now solve eq. (15) by resolving the vibration into a series of natural modes, and we put

$$v(x, t) = \sum_{k=1}^{\infty} v_{(k)}(t) v_{(k)}(x), \quad (16)$$

<sup>3)</sup> The method is described in detail in 1).

$$p(x, t) = \sum_{k=1}^{\infty} \mu p_{(k)}(t) v_{(k)}(x), \quad (17)$$

$$p_{(k)}(t) = \frac{\sum_0^l \int p(x, t) v_{(k)}(x) dx}{\sum_0^l \int \mu v_{(k)}^2(x) dx}, \quad (18)$$

where

$v_{(k)}(t)$  is the generalised co-ordinate of the deflection, as a time function.

$p_{(k)}(t)$  is the generalised co-ordinate of the load.

The summation  $\Sigma$  is to be extended over all the spans of the system.

On inserting from eqs. (16) to (18) into eq. (15) and considering that

$E J \frac{d^4 v_{(k)}(x)}{dx^4} = \mu \omega_{(k)}^2 v_{(k)}(x)$  for any  $k$  we obtain

$$\frac{d^2 v_{(k)}(t)}{dt^2} + 2 \omega_b \frac{d v_{(k)}(t)}{dt} + \omega_{(k)}^2 v_{(k)}(t) = p_{(k)}(t). \quad (19)$$

If the force  $P \sin \Omega t$  is acting at the point  $x = a = ct$  we have acc. to (4) and (18):

$$p_{(k)}(t) = \frac{P}{\sum_0^l \int \mu v_{(k)}^2(x) dx} \sin \Omega t (C_1 \cosh \omega t + C_2 \sinh \omega t + C_3 \cos \omega t + C_4 \sin \omega t), \quad (20)$$

where  $\omega = \frac{\lambda c}{l}$ , and the constants  $C$  are determined by eqs. (6) to (14).

Inserting for  $p_{(k)}(t)$  from (20) into (19) we obtain a differential equation, the particular integral of which can be expressed in the form

$$\begin{aligned} v_{(k)}(t) = & \bar{\mathfrak{C}}_1 \sin \Omega t \cosh \omega t + \bar{\mathfrak{C}}_2 \sin \Omega t \sinh \omega t + \bar{\mathfrak{C}}_3 \cos \Omega t \cosh \omega t + \\ & + \bar{\mathfrak{C}}_4 \cos \Omega t \sinh \omega t + \mathfrak{C}_1 \sin \Omega t \cos \omega t + \mathfrak{C}_2 \sin \Omega t \sin \omega t + \\ & + \mathfrak{C}_3 \cos \Omega t \cos \omega t + \mathfrak{C}_4 \cos \Omega t \sin \omega t. \end{aligned} \quad (21)$$

Substituting for  $v_{(k)}(t)$  from eq. (21) into eq. (19) and rearranging we have

$$\begin{aligned} & [\bar{\mathfrak{C}}_1 (\omega^2 - \Omega^2) - 2 \bar{\mathfrak{C}}_4 \omega \Omega + 2 \bar{\mathfrak{C}}_2 \omega \omega_b - 2 \bar{\mathfrak{C}}_3 \Omega \omega_b + \bar{\mathfrak{C}}_1 \omega_{(k)}^2] \sin \Omega t \cosh \omega t + \\ & + [\bar{\mathfrak{C}}_2 (\omega^2 - \Omega^2) - 2 \bar{\mathfrak{C}}_3 \omega \Omega + 2 \bar{\mathfrak{C}}_1 \omega \omega_b - 2 \bar{\mathfrak{C}}_4 \Omega \omega_b + \bar{\mathfrak{C}}_2 \omega_{(k)}^2] \sin \Omega t \sinh \omega t + \\ & + [\bar{\mathfrak{C}}_3 (\omega^2 - \Omega^2) + 2 \bar{\mathfrak{C}}_2 \omega \Omega + 2 \bar{\mathfrak{C}}_4 \omega \omega_b + 2 \bar{\mathfrak{C}}_1 \Omega \omega_b + \bar{\mathfrak{C}}_3 \omega_{(k)}^2] \cos \Omega t \cosh \omega t + \\ & + [\bar{\mathfrak{C}}_4 (\omega^2 - \Omega^2) + 2 \bar{\mathfrak{C}}_1 \omega \Omega + 2 \bar{\mathfrak{C}}_3 \omega \omega_b + 2 \bar{\mathfrak{C}}_2 \Omega \omega_b + \bar{\mathfrak{C}}_4 \omega_{(k)}^2] \cos \Omega t \sinh \omega t + \\ & + [-\bar{\mathfrak{C}}_1 (\omega^2 - \Omega^2) - 2 \bar{\mathfrak{C}}_4 \omega \Omega + 2 \bar{\mathfrak{C}}_2 \omega \omega_b - 2 \bar{\mathfrak{C}}_3 \Omega \omega_b + \bar{\mathfrak{C}}_1 \omega_{(k)}^2] \sin \Omega t \cos \omega t + \\ & + [-\bar{\mathfrak{C}}_2 (\omega^2 - \Omega^2) + 2 \bar{\mathfrak{C}}_3 \omega \Omega - 2 \bar{\mathfrak{C}}_1 \omega \omega_b - 2 \bar{\mathfrak{C}}_4 \Omega \omega_b + \bar{\mathfrak{C}}_2 \omega_{(k)}^2] \sin \Omega t \sin \omega t + \\ & + [-\bar{\mathfrak{C}}_3 (\omega^2 - \Omega^2) + 2 \bar{\mathfrak{C}}_2 \omega \Omega + 2 \bar{\mathfrak{C}}_4 \omega \omega_b + 2 \bar{\mathfrak{C}}_1 \Omega \omega_b + \bar{\mathfrak{C}}_3 \omega_{(k)}^2] \cos \Omega t \cos \omega t + \\ & + [-\bar{\mathfrak{C}}_4 (\omega^2 - \Omega^2) - 2 \bar{\mathfrak{C}}_1 \omega \Omega - 2 \bar{\mathfrak{C}}_3 \omega \omega_b + 2 \bar{\mathfrak{C}}_2 \Omega \omega_b + \bar{\mathfrak{C}}_4 \omega_{(k)}^2] \cos \Omega t \sin \omega t = \\ & = \frac{P}{\sum_0^l \int \mu v_{(k)}^2(x) dx} [C_1 \sin \Omega t \cosh \omega t + C_2 \sin \Omega t \sinh \omega t + C_3 \sin \Omega t \cos \omega t + \\ & + C_4 \sin \Omega t \sin \omega t]. \end{aligned} \quad (22)$$

The constants  $\mathfrak{C}$  and  $\bar{\mathfrak{C}}$  are determined from the condition that the coefficients of identical products ( $\sin \Omega t \cosh \omega t$ , etc.) have to be equal<sup>4</sup>).

The calculation is simplified in the case that the frequency of the moving force is in resonance with the frequency of the first natural mode. In this case it is sufficient to take into account only the first terms in the series as expressed by eqs. (16) and (17). In addition we may in almost all cases suppose the values of  $\omega_b$  and  $\omega$  to be small in comparison with  $\Omega$ . Making these assumptions we obtain (for  $k=1$ ):

$$\begin{aligned}\mathfrak{C}_1 &\cong \mathfrak{C}_2 \cong \bar{\mathfrak{C}}_1 \cong \bar{\mathfrak{C}}_2 \cong 0, \\ \mathfrak{C}_3 &= \epsilon (C_4 \omega - C_3 \omega_b), \\ \mathfrak{C}_4 &= \epsilon (-C_3 \omega - C_4 \omega_b), \\ \bar{\mathfrak{C}}_3 &= \bar{\epsilon} (C_1 \omega_b - C_2 \omega), \\ \bar{\mathfrak{C}}_4 &= \bar{\epsilon} (C_2 \omega_b - C_1 \omega),\end{aligned}\tag{23}$$

where

$$\begin{aligned}\epsilon &= \frac{P}{2\Omega(\omega^2 + \omega_b^2) \sum_0^l \int \mu v_{(k)}^2(x) dx}, \\ \bar{\epsilon} &= \frac{P}{2\Omega(\omega^2 - \omega_b^2) \sum_0^l \int \mu v_{(k)}^2(x) dx}.\end{aligned}\tag{24}$$

Eq. (21) is only a particular integral of (19) and it does not satisfy the initial time-conditions of the movement. To satisfy these conditions we have to add another term which expresses the natural damped vibrations of the system oscillating in the  $k$ -th natural mode (usually we consider only  $k=1$ ). If the damping is slight the term which has to be added is given by the formula

$$v_{0(k)}(t) = C_0 e^{-\omega_b t} (\cos \varphi_0 \sin \omega_{(k)} t + \sin \varphi_0 \cos \omega_{(k)} t),\tag{25}$$

where by  $C_0$  and  $\varphi_0$  we denoted the constants of integration. The final value of the generalised co-ordinate of the deflection is thus

$$v_{(k)}(t)_{fin} = v_{(k)}(t) + v_{0(k)}(t).\tag{26}$$

If the initial conditions of the movement are given by  $v_{(k)}(0)_{fin}$  and  $\frac{dv_{(k)}(0)_{fin}}{dt}$ , we obtain for  $t=0$  from eqs. (25), (26) and (21)

$$C_0 \sin \varphi_0 = -\mathfrak{C}_3 - \bar{\mathfrak{C}}_3 + v_{(k)}(0)_{fin}\tag{27}$$

$$C_0 \cos \varphi_0 = \frac{dv_{(k)}(0)_{fin}}{dt} \frac{1}{\omega_{(k)}}.\tag{28}$$

<sup>4</sup>) The calculation is given in 1), chap. VIII, 2 and 3.

<sup>5</sup>) It is obvious that this simplification would not be possible for  $\omega = \omega_b$ . In practical cases, however, we almost always have  $\omega > \omega_b$ .

The expression for  $v_{(k)}(t)_{fin}$  appears thus in the form

$$v_{(k)}(t)_{fin} = \cos \Omega t [\mathfrak{C}_3 \cos \omega t + \mathfrak{C}_4 \sin \omega t + \bar{\mathfrak{C}}_3 \cosh \omega t + \bar{\mathfrak{C}}_4 \sinh \omega t] - \tag{29}$$

$$- e^{-\omega t} \left\{ [(\mathfrak{C}_3 + \bar{\mathfrak{C}}_3) - v_{(k)}(0)_{fin}] \cos \Omega t - \frac{1}{\Omega} \frac{d v_{(k)}(0)_{fin}}{d t} \sin \Omega t \right\}.$$

We have now to determine the integrals in the denominators of the formulæ (24).

If the bar  $K, K + 1$  is continuous at both ends, the constants of integration in eq. (4) are given by eqs. (6), (7) and (8) and we have <sup>6)</sup>

$$\int \mu v_{(k)}^2(x) dx = \frac{E J}{\omega_{(k)}^2} \left[ \frac{\gamma_K^2 + \gamma_{K+1}^2}{l} \Phi_2(\lambda) + \frac{2 \gamma_K \gamma_{K+1}}{l} \Phi_1(\lambda) \right], \tag{30}$$

where the functions  $\Phi$  are defined as follows

$$\Phi_1(\lambda) = \frac{1}{4} [F_1(\lambda) F_2(\lambda) - F_3(\lambda) - F_1(\lambda)], \tag{31}$$

$$\Phi_2(\lambda) = \frac{1}{4} [F_1^2(\lambda) - F_2(\lambda)]. \tag{32}$$

If the bar  $K, K + 1$  is hinged at the end  $K$  we make use of eqs. (4), (9), (10) and (11) and obtain

$$\int \mu v_{(k)}^2(x) dx = \frac{E J}{\omega_{(k)}^2} \frac{\gamma_{K+1}^2}{l} \Phi_7(\lambda), \tag{33}$$

where

$$\Phi_7(\lambda) = \frac{1}{4} [-F_7(\lambda) + F_7^2(\lambda) + 2 F_9(\lambda)]. \tag{34}$$

If the hinge is at the point  $K + 1$  we put in eq. (33) simply  $\gamma_K$  instead of  $\gamma_{K+1}$ .

In the analysis as described above we have neglected the fact, that simultaneously with the pulsating force also the mass of the locomotive is moving along the bridge, and that the vibrations are thus affected by inertia forces of the mass of the engine. We can approximately account for this <sup>7)</sup> if we assume the inertial mass  $m_L$  of the locomotive to be steadily placed in the point  $x = s$  where we expect the largest deflection to occur. The inertial force of the mass  $m_L = \frac{W_L}{g}$  is given by the formula

$$- m_L \frac{d^2 v(s, t)}{d t^2}.$$

This force may be also expanded in a series acc. to eq. (17). Considering only the first term in the series we obtain acc. to eqs. (16) and (18) a substitute load-function <sup>8)</sup>:

$$h(x, t) = - m_L \frac{d^2 v_{(1)}(t)}{d t^2} \frac{\mu v_{(1)}(x)}{\sum_0^l \mu v_{(1)}^2(x) dx} v_{(1)}^2(s).$$

<sup>6)</sup> See ref. 1); eqs. (83) to (86).

<sup>7)</sup> A similar method has been used by INGLIS for simply supported beams. (INGLIS, "A Mathematical Treatise on Vibrations in Railway Bridges", Cambridge 1934.)

<sup>8)</sup> See ref. 1), eqs. (240) to (243).

This load-function represents the inertia force of uniformly distributed mass

$$\mu m_L \frac{v_{(1)}^2(s)}{\sum_0^l \int \mu v_{(1)}^2(x) dx}.$$

The system is in this case oscillating as if it were loaded by the mass

$$\bar{\mu} = \mu \left[ 1 + m_L \frac{v_{(1)}^2(s)}{\sum_0^l \int \mu v_{(1)}^2(x) dx} \right]. \quad (35)$$

## II. Application of the theoretical solution to the experimentally tested actual structure

The main girders of the tested bridge are continuous over three spans of 60.8, 77.4, and 60.8 m, respectively. The girders are open-web parallel-boom trusses with simple triangle bracing. Along the individual spans the cross sections of the trusses are variable.

An exact solution of such a type of structure would present unusual difficulties. For dynamical analysis, therefore, the two main girders have been replaced by a substitute single continuous truss with cross sections constant within the individual spans. The moments of inertia for this substitute system have been determined in such a manner, that both the actual and the substitute systems have the same maximum deflections  $\tilde{v}_e$  and  $\tilde{v}_s$  if loaded as shown in fig. 1. The values of the moments of inertia thus obtained are  $2,08 m^4$  and  $3,14 m^4$  for the end and middle spans respectively.

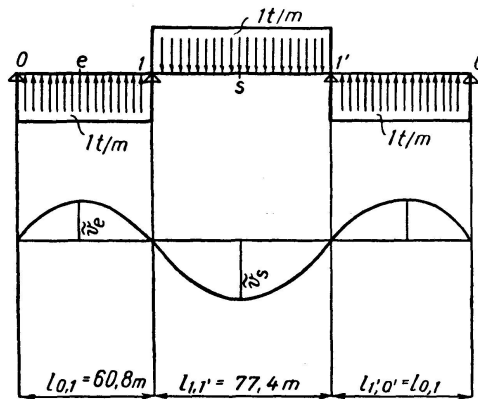


Fig. 1. Equivalent Load for the Substitute Beam.

The influence line for the deflection at the centre "s" of the middle span (fig. 2) has been taken to be the same as resulted from the statical analysis, the ordinates have been, however, corrected according to the results obtained at the load test, so that the line does not exactly correspond to the above specified substitute truss.

The weight of the bridge is 5.5 t per linear meter.

The basic values are thus given as follows:

$$l_{0,1} = 60,8 \text{ m}, \quad J_{0,1} = 2,08 \text{ m}^4, \quad \mu_{0,1} = 5,5/9,81 = 0,560 \text{ t m}^{-2} \text{ s}^2,$$

$$l_{1,1'} = 77,4 \text{ m}, \quad J_{1,1'} = 3,14 \text{ m}^4, \quad \mu_{1,1'} = 5,5/9,81 = 0,560 \text{ t m}^{-2} \text{ s}^2.$$

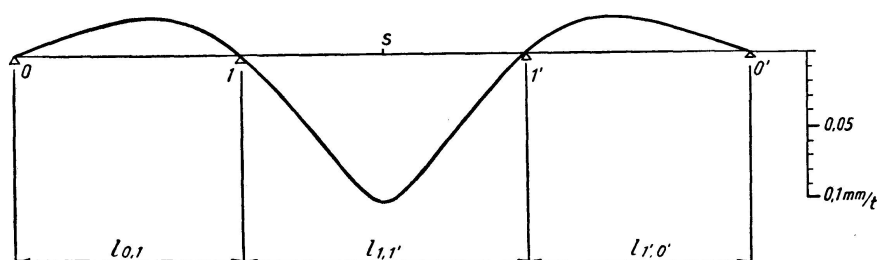


Fig. 2. Influence Line for Deflection at Middle-Span Centre.

Further we have

$$\frac{\lambda_{1,1'}}{\lambda_{0,1}} = \frac{l_{1,1'}^4}{l_{0,1}^4} \sqrt{\frac{J_{0,1}}{J_{1,1'}}} = 1,150.$$

The natural frequency of symmetrical vibrations is calculated acc. to eq. (1)<sup>9)</sup>, with respect to eqs. (2) and (3):

$$\frac{J_{0,1}}{l_{0,1}} F_7(\lambda_{0,1}) = \frac{J_{1,1'}}{l_{1,1'}} [F_1(\lambda_{1,1'}) - F_2(\lambda_{1,1'})]. \quad (36)$$

The lowest values for which eq. (36) holds true are

$$\lambda_{0,1} = 2,93, \quad \lambda_{1,1'} = 3,37.$$

The fundamental natural angular frequency is given by the formula

$$\omega_{(1)} = \frac{\lambda_{1,1'}^2}{l_{1,1'}^2} \sqrt{\frac{E J_{1,1'}}{\mu_{1,1'}}} = \frac{3,37^2}{77,4^2} \sqrt{\frac{21 \cdot 10^6 \cdot 3,14}{0,560}} = 20,5 \text{ s}^{-1},$$

so that for the frequency of the load-free bridge we obtain

$$n_{(1)} = \frac{20,5}{2\pi} = 3,26 \text{ s}^{-1}.$$

If we assume for the amplitudes  $\gamma_1 = -\gamma_{1'} = 1$  we obtain from equations (30) to (34)

<sup>9)</sup> See ref. 1), chap. II, eq. (52).

$$\begin{aligned}
\sum_0 \int \mu v_{(1)}^2(x) dx &= \frac{E}{\omega_{(1)}^2} \left\{ \frac{2J_{0,1}}{l_{0,1}} \frac{1}{4} [-F_7(\lambda_{0,1}) + F_7^2(\lambda_{0,1}) + 2F_9(\lambda_{0,1})] + \right. \\
&\quad \left. + \frac{2J_{1,1'}}{l_{1,1'}} \frac{1}{4} [F_1^2(\lambda_{1,1'}) - F_2(\lambda_{1,1'}) - F_1(\lambda_{1,1'}) F_2(\lambda_{1,1'}) + F_3(\lambda_{1,1'}) + F_1(\lambda_{1,1'})] \right\} = \\
&= \frac{21 \cdot 10^6}{20,5^2} \left[ \frac{2,08}{60,8 \cdot 2} (-1,035 + 1,035^2 + 2 \cdot 5,536) + \right. \\
&\quad \left. + \frac{3,14}{77,4 \cdot 2} (3,274^2 - 2,409 - 3,274 \cdot 2,409 + 11,621 + 3,274) \right] \cong 25200 \text{ tms}^2.
\end{aligned}$$

The first natural mode is then expressed by eq. (4). With respect to  $\gamma_1 = -\gamma_{1'} = 1$  we obtain now for the first span the constants of integration acc. to eqs. (9), (10), and (11).

$$C_1 = C_3 = 0,$$

$$C_2 = \frac{l_{0,1}}{\lambda_{0,1}} \frac{\sin \lambda_{0,1}}{\cosh \lambda_{0,1} \sin \lambda_{0,1} - \sinh \lambda_{0,1} \cos \lambda_{0,1}} = \frac{60,8}{2,93} \frac{0,210}{11,10} = 0,393,$$

$$C_4 = -\frac{l_{0,1}}{\lambda_{0,1}} \frac{\sinh \lambda_{0,1}}{\cosh \lambda_{0,1} \sin \lambda_{0,1} - \sinh \lambda_{0,1} \cos \lambda_{0,1}} = -\frac{60,8}{2,93} \frac{9,34}{11,10} = -17,45.$$

$$\text{Thus} \quad v_{(1)}(x) = 0,393 \sinh 2,93 \frac{x}{l} - 17,45 \sin 2,93 \frac{x}{l}. \quad (37)$$

For the second span we have, acc. to eqs. (6), (7) and (8):

$$C_1 = -C_3 = -\frac{l_{1,1'}}{2\lambda_{1,1'}^2} [F_2(\lambda_{1,1'}) - F_1(\lambda_{1,1'})] = -\frac{77,4}{2 \cdot 3,37^2} (2,409 - 3,274) = 2,94,$$

$$\begin{aligned}
C_2 &= -\frac{l_{1,1'}}{2\lambda_{1,1'}^3} [F_4(\lambda_{1,1'}) + F_3(\lambda_{1,1'})] + \frac{l_{1,1'}}{2\lambda_{1,1'}} = \\
&= -\frac{77,4}{2 \cdot 3,37^3} (2,461 + 11,621) + \frac{77,4}{2 \cdot 3,37} = -2,87,
\end{aligned}$$

$$C_4 = -C_2 + \frac{l_{1,1'}}{\lambda_{1,1'}} = 2,87 + \frac{77,4}{3,37} = 25,83,$$

$$v_{(1)}(x) = 2,94 \cosh 3,37 \frac{x}{l} - 2,87 \sinh 3,37 \frac{x}{l} - 2,94 \cos 3,37 \frac{x}{l} + 25,83 \sin 3,37 \frac{x}{l}. \quad (38)$$

For the centre "s" of the middle span we obtain

$$\begin{aligned}
v_{(1)}\left(\frac{l_{1,1'}}{2}\right) &= 2,94 \cosh 1,685 - 2,87 \sinh 1,685 - 2,94 \cos 1,685 + \\
&\quad + 25,83 \sin 1,685 = 26,69.
\end{aligned}$$

For the third span we determine the constants of integration acc. to eqs. (12), (13), and (14) as follows

$$C_1 = -C_3 = \frac{l_{0,1}}{2\lambda_{0,1}^2} F_7(\lambda_{0,1}) = \frac{60,8}{2 \cdot 2,93^2} 1,035 = 3,67,$$

$$C_2 = \frac{l_{0,1}}{2\lambda_{0,1}^3} F_9(\lambda_{0,1}) - \frac{l_{0,1}}{2\lambda_{0,1}} = \frac{60,8}{2 \cdot 2,93^2} 5,536 - \frac{60,8}{2 \cdot 2,93} = -3,68,$$

$$C_4 = -C_2 - \frac{l_{0,1}}{\lambda_{0,1}} = 3,68 - \frac{60,8}{2,93} = -17,04,$$

so that we have

$$v_{(1)}(x) = 3,67 \cosh 2,93 \frac{x}{l} - 3,68 \sinh 2,93 \frac{x}{l} - 3,67 \cos 2,93 \frac{x}{l} - 17,04 \sin 2,93 \frac{x}{l}. \quad (39)$$

The first natural mode of vibration as expressed by eq. (39) is shown in fig. 3a.

The "angular frequency" of the damping has been estimated to be  $\omega_b = 0,3s^{-1}$ .

At the load test the bridge has been moved upon by a two-cylinder, 97-ton locomotive, with five coupled driving axles, the centrifugal forces produced

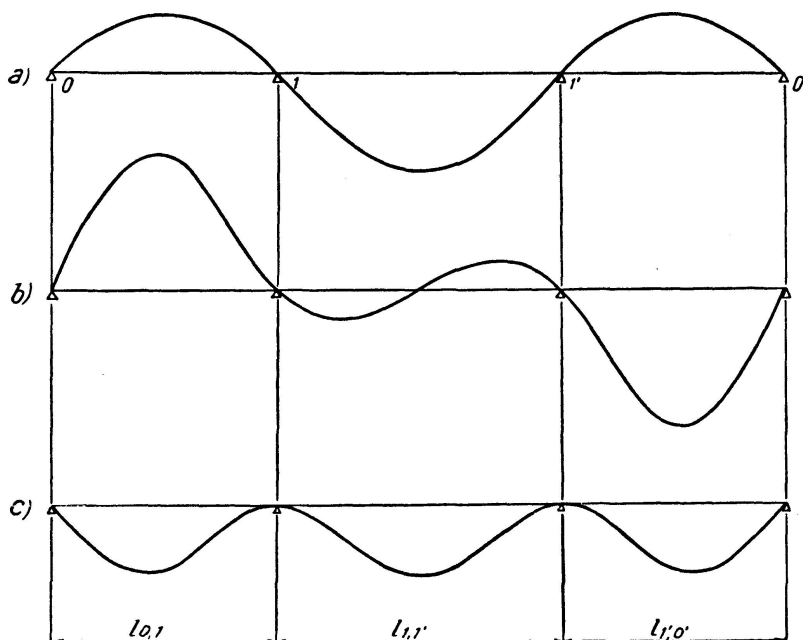


Fig. 3.

- a) First Natural Mode of Vibration.
- b) Second Natural Mode of Vibration.
- c) Third Natural Mode of Vibration.

having the value of  $0.3 N^2$  (in tons, if  $N$  denotes the number of revolutions per second). The circumference of the driving wheels was 3.96 m.

The dynamical effects produced by the locomotive we shall now investigate in the manner described in Part I of this paper. We assume the inertial mass of the engine to be constantly placed at the centre of the middle span, i. e. we neglect the movement of the inertial mass and take into consideration only the movement of the weight  $W_L$  and of the centrifugal forces of the engine along the bridge.

The effect produced by the movement of the weight along the bridge is expressed with sufficient accuracy by the statical effects only.

In fig. 2 the influence line for the deflection of the point "s" at the centre of the middle span is shown. Evaluating the line using the axle-loads of the engine we obtain the curve of variation for the deflection of the point "s", produced by the locomotive crossing the bridge at practically any speed, but on the assumption that the centrifugal forces of the driving axles are non-acting. Thus we obtain the curve shown in fig. 4a.

When calculating the effects of the moving periodical forces of the driving axles we shall consider only the case when  $N = \bar{n}_{(1)}$ , where  $\bar{n}_{(1)}$  denotes the first natural frequency of the loaded bridge. The angular frequency of the loaded bridge is

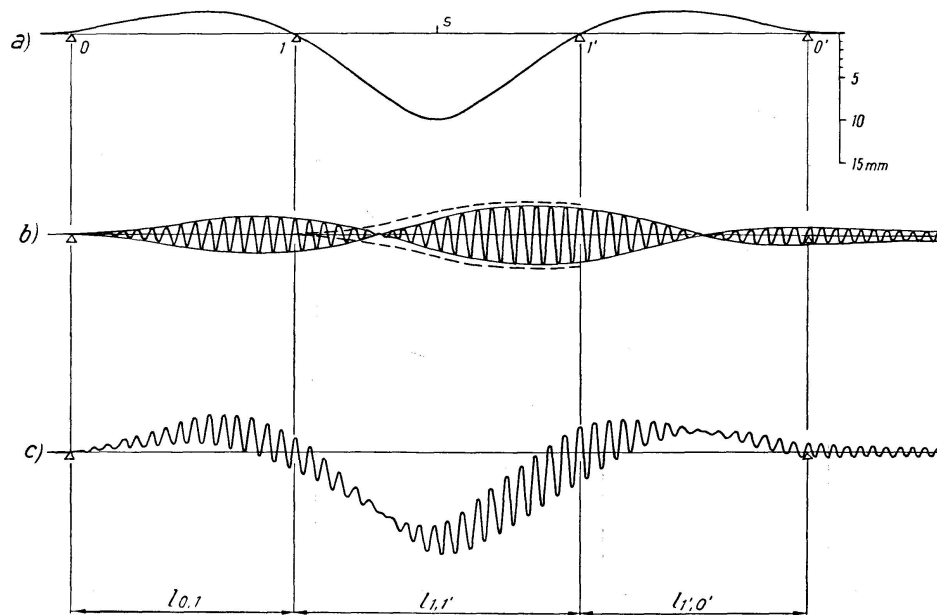


Fig. 4.

- a) Statical Deflection of Centre of Middle Span Produced by a 97-t Locomotive.  
 b) Dynamical Deflection Produced by a Moving Alternating Force, the Frequency of which is in Resonance with the First Natural Frequency of the System. (Dotted Line is the Envelope Curve of the Amplitudes for the Case that the Force is Moving only along the Middle Span.)  
 c) Theoretical Curve for Dynamical Deflection of Centre of Middle Span.

$$\bar{\omega}_{(1)}^2 = \omega_{(1)}^2 \frac{\mu}{\bar{\mu}},$$

where, according to eq. (35)

$$\frac{\bar{\mu}}{\mu} = 1 + \frac{m_L v_{(1)}^2(s)}{\sum_0^l \int \mu v_{(1)}^2(x) dx} = 1 + \frac{97 \cdot 26,69^2}{9,81 \cdot 25200} = 1,28.$$

Thus we have 
$$\bar{\omega}_{(1)} = \sqrt{\frac{20,5^2}{1,28}} = 18,1 \text{ s}^{-1}$$

and 
$$\bar{n}_{(1)} = \frac{18,1}{2\pi} = 2,88 \text{ s}^{-1}.$$

The critical speed is

$$c = 2,88 \cdot 3,96 = 11,4 \text{ m s}^{-1} \cong 41 \text{ km p. h.}$$

and the corresponding centrifugal force

$$P = 0,3 \cdot 2,88^2 = 2,49 \text{ t.}$$

We have also

$$\bar{\omega}_b = \omega_b \frac{\mu}{\bar{\mu}} = \frac{0,3}{1,28} = 0,235 \text{ s}^{-1}$$

and 
$$\sum_0^l \int \bar{\mu} v_{(1)}^2(x) dx = 1,28 \cdot 25200 = 32300 \text{ t ms}^2.$$

Further calculation is carried out as described in Part I of this paper<sup>10</sup>).

For the span 0,1 we have

$$\omega = \frac{\lambda_{0,1} c}{l_{0,1}} = \frac{2,93 \cdot 11,4}{60,8} = 0,549 \text{ s}^{-1}$$

and, acc. to eqs. (23) and (24)

$$\epsilon = \frac{P}{2 \bar{\omega}_{(1)} (\omega^2 + \bar{\omega}_b^2) \sum_0^l \int \bar{\mu} v_{(1)}^2(x) dx} = \frac{2,49}{2 \cdot 18,1 (0,549^2 + 0,235^2) 32300} = 0,598 \cdot 10^{-5},$$

$$\mathfrak{C}_3 = \epsilon C_4 \omega = -0,598 \cdot 10^{-5} \cdot 17,45 \cdot 0,549 = -5,74 \cdot 10^{-5},$$

$$\mathfrak{C}_4 = -\epsilon C_4 \bar{\omega}_b = 0,598 \cdot 10^{-5} \cdot 17,45 \cdot 0,235 = 2,45 \cdot 10^{-5},$$

$$\bar{\epsilon} = \frac{P}{2 \bar{\omega}_{(1)} (\omega^2 - \bar{\omega}_b^2) \sum_0^l \int \bar{\mu} v_{(1)}^2(x) dx} = \frac{2,49}{2 \cdot 18,1 (0,549^2 - 0,235^2) 32300} = 0,865 \cdot 10^{-5},$$

$$\bar{\mathfrak{C}}_3 = -\bar{\epsilon} C_2 \omega = -0,865 \cdot 10^{-5} \cdot 0,393 \cdot 0,549 = -0,1865 \cdot 10^{-5},$$

$$\bar{\mathfrak{C}}_4 = \bar{\epsilon} C_2 \bar{\omega}_b = 0,865 \cdot 10^{-5} \cdot 0,393 \cdot 0,235 = 0,0798 \cdot 10^{-5}.$$

When the harmonically varying force is moving along the span 0,1 we obtain the curve of variation for the deflection of the point "s" at the centre of the middle span acc. to eqs. (29) and (16). Considering only the first term in the series we have

<sup>10</sup>) For more extensive information see ref. 1), numerical example 22.

$$v\left(\frac{l_{1,1'}}{2}, t\right) = \cos \omega_{(1)} t \cdot A(t), \quad (40)$$

where

$$A(t) = v_{(1)}\left(\frac{l_{1,1'}}{2}\right) [\mathfrak{C}_3 (\cos \omega t - e^{-\bar{\omega}_b t}) + \mathfrak{C}_4 \sin \omega t + \bar{\mathfrak{C}}_3 (\cosh \omega t - e^{-\bar{\omega}_b t}) + \bar{\mathfrak{C}}_4 \sinh \omega t] \quad (41)$$

denotes the envelope of the deflections of the point "s". Formula (40) holds true in the case that at the moment of entering the bridge the centrifugal force is acting vertically downwards. In a general case we have

$$v = \left(\frac{l_{1,1'}}{2}, t\right) = \cos(\omega_{(1)} t + \varphi_p) \cdot A(t).$$

The envelope curve  $A(t)$  is, however, the same for any value of the phase difference  $\varphi_p$  of the exciting force. On introducing numerical values into eq. (41) we obtain

$$A(t) = 26,69 \cdot 10^{-5} [-5,74 (\cos 0,549 t - e^{-0,235 t}) + 2,45 \sin 0,549 t - 0,1865 (\cosh 0,549 t - e^{-0,235 t}) + 0,0798 \sinh 0,549 t]. \quad (42a)$$

Putting  $t = \frac{x}{c}$ ,  $\omega t = \lambda_{0,1} \frac{x}{l}$  and rearranging we have

$$A(x) = \left[ -153 \left( \cos 2,93 \frac{x}{l} - e^{-1,252 x/l} \right) + 65,4 \sin 2,93 \frac{x}{l} - 4,97 \left( \cosh 2,93 \frac{x}{l} - e^{-1,252 x/l} \right) + 2,1 \sinh 2,93 \frac{x}{l} \right] 10^{-5}. \quad (42b)$$

For  $x = l_{0,1}$  we obtain

$$A(l_{0,1}) = 180 \cdot 10^{-5}.$$

When the harmonically varying force moves along the middle span we obtain in a similar manner

$$\omega = \frac{3,37 \cdot 11,4}{77,4} = 0,496 \text{ s}^{-1},$$

$$\epsilon = \frac{2,49}{2 \cdot 18,1 (0,496^2 + 0,235^2) 32300} = 0,707 \cdot 10^{-5},$$

$$\mathfrak{C}_3 = \epsilon (C_4 \omega - C_3 \bar{\omega}_b) = 0,707 \cdot 10^{-5} (25,83 \cdot 0,496 + 2,94 \cdot 0,235) = 9,54 \cdot 10^{-5},$$

$$\mathfrak{C}_4 = \epsilon (-C_3 \omega - C_4 \bar{\omega}_b) = 0,707 \cdot 10^{-5} (2,94 \cdot 0,496 - 25,83 \cdot 0,235) = -3,26 \cdot 10^{-5},$$

$$\bar{\epsilon} = \frac{2,49}{2 \cdot 18,1 (0,496^2 - 0,235^2) 32300} = 1,115 \cdot 10^{-5},$$

$$\bar{\mathfrak{C}}_3 = \bar{\epsilon} (C_1 \bar{\omega}_b - C_2 \omega) = 1,115 \cdot 10^{-5} (2,94 \cdot 0,235 + 2,87 \cdot 0,496) = 2,36 \cdot 10^{-5},$$

$$\bar{\mathfrak{C}}_4 = \bar{\epsilon} (C_2 \bar{\omega}_b - C_1 \omega) = 1,115 \cdot 10^{-5} (-2,87 \cdot 0,235 - 2,94 \cdot 0,496) = -2,38 \cdot 10^{-5}.$$

For the deflection of the point "s" we have

$$A(t) = 26,69 \cdot 10^{-5} [9,54 (\cos 0,496 t - e^{-0,235 t}) - 3,26 \sin 0,496 t + 2,36 (\cosh 0,496 t - e^{-0,235 t}) - 2,38 \sinh 0,496 t] + A(l_{0,1}) e^{-0,235 t}, \quad (43 a)$$

$$A(x) = \left[ 255 \left( \cos 3,37 \frac{x}{l} - e^{-1,595 x/l} \right) - 87,0 \sin 3,37 \frac{x}{l} + 63,0 \left( \cosh 3,37 \frac{x}{l} - e^{-1,595 x/l} \right) - 63,4 \sinh 3,37 \frac{x}{l} + 180 e^{-1,595 x/l} \right] 10^{-5}. \quad (43 b)$$

The last term in eqs. (43) denotes residual oscillation which remains after the moving force had passed the span 0,1. Putting  $x=l_{1,1'}$  we obtain

$$A(l_{1,1'}) = -298 \cdot 10^{-5}.$$

Finally when the force is crossing the span 1', 0' we have<sup>11)</sup>:

$$\omega = 0,549 \text{ s}^{-1},$$

$$\epsilon = 0,598 \cdot 10^{-5} \quad (\text{as in the span } 0,1),$$

$$\mathfrak{C}_3 = \epsilon (C_4 \omega - C_3 \bar{\omega}_b) = 0,598 \cdot 10^{-5} (-17,04 \cdot 0,549 + 3,67 \cdot 0,235) = -0,508 \cdot 10^{-5},$$

$$\mathfrak{C}_4 = \epsilon (-C_3 \omega - C_4 \bar{\omega}_b) = 0,598 \cdot 10^{-5} (3,67 \cdot 0,549 + 17,04 \cdot 0,235) = 3,60 \cdot 10^{-5},$$

$$\bar{\epsilon} = 0,865 \cdot 10^{-5},$$

$$\bar{\mathfrak{C}}_3 = \bar{\epsilon} (C_1 \bar{\omega}_b - C_2 \omega) = 0,865 \cdot 10^{-5} (3,67 \cdot 0,235 + 3,68 \cdot 0,549) = 2,49 \cdot 10^{-5},$$

$$\bar{\mathfrak{C}}_4 = \bar{\epsilon} (C_2 \bar{\omega}_b - C_1 \omega) = 0,865 \cdot 10^{-5} (-3,68 \cdot 0,235 - 3,67 \cdot 0,549) = -2,49 \cdot 10^{-5},$$

$$A(t) = 26,69 \cdot 10^{-5} [-5,08 (\cos 0,549 t - e^{-0,235 t}) + 3,60 \sin 0,549 t + 2,49 (\cosh 0,549 t - e^{-0,235 t}) - 2,49 \sinh 0,549 t] + A(l_{1,1'}) e^{-0,235 t}, \quad (44 a)$$

$$A(x) = \left[ -135,5 \left( \cos 2,93 \frac{x}{l} - e^{-1,252 x/l} \right) + 96,0 \sin 2,93 \frac{x}{l} + 66,5 \left( \cosh 2,93 \frac{x}{l} - e^{-1,252 x/l} \right) - 66,5 \sinh 2,93 \frac{x}{l} - 298 e^{-1,252 x/l} \right] 10^{-5}. \quad (44 b)$$

The deflection as expressed by eqs. (42 b) to (44 b) is graphically represented in fig. 4 b. If we superimpose the curve of fig. 4 b upon the curve of fig. 4 a, we obtain the curve given in fig. 4 c, which shows the variation of the deflection of the point "s" if the locomotive crosses the bridge at critical speed.

The theoretical analysis given above is only approximate, as it is impossible for the state of resonance to last for the full time interval of the locomotive crossing the bridge. The natural frequency of the loaded bridge being dependent on the position of the mass of the locomotive, it varies within

<sup>11)</sup> In numerical example 22, chap. VIII/3 of the book<sup>1)</sup> it has been incorrectly assumed that the constants for the span 0,1 are the same as for the span 1', 0'. This faulty assumption affects, however, the results only slightly.

rather wide limits. If the state of resonance were to last for the full time interval of the engine crossing the bridge, the speed of the movement would have to vary. These considerations give rise to the question if the residual vibration which remains after the engine had passed the end span has to be considered at all.

The numerical example had therefore been re-calculated, again approximately, on the assumption that resonance lasts only for the full time interval of the engine crossing the middle span, and the dynamical effects produced while crossing the end span were neglected altogether. This assumption results again in eq. (43), where, however, the last term is missing. Graphical representation for this case is given in fig. 5.

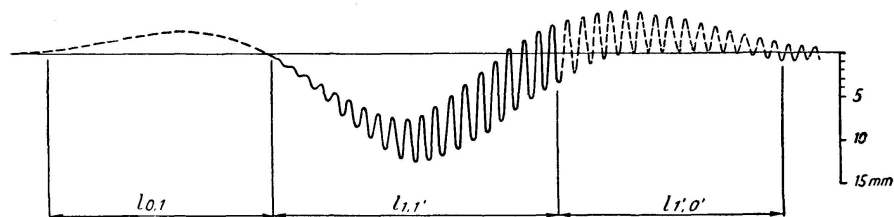


Fig. 5. Theoretical Curve for Dynamical Deflection for the Case that the Alternating Forces of Axles are Acting only when Moving along the Middle-Span.

### III. Results of Load-Tests

The 97-ton locomotive used for the tests had been driven across the bridge at various speeds. The produced dynamical effects have been measured at different points of the structure by means of strain-gages and deflection meters. In figs. 6 to 12 we give the diagrams obtained with the deflection meters

Fig. 6. Deflection of Centre of Middle-Span Recorded by the Geiger-Instrument during the Crossing of a Two-Cylinder Locomotive, Driving at 31 km p. h.

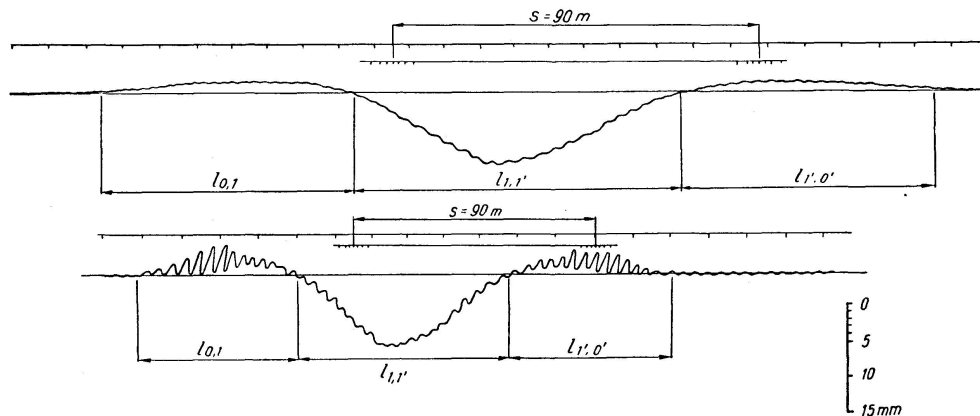


Fig. 7. Recorded Deflection of the Centre of Middle-Span, Locomotive Driving at 49.5 km p. h.

applied at the centre of the middle span, i. e. at the point which had been also theoretically investigated.

Figs. 6 to 11 show that the dynamical effects produced by the moving periodical forces are distinctly dependent on the velocity of the movement. For 31 km p. h. (fig. 6) the effects are hardly perceivable, but for 37 km p. h. (fig. 8) the effects attain already considerable values. Pronounced resonance effects are to be distinguished still for the speed of 44 km p. h. (fig. 10), and only for 49 km p. h. (fig. 7) the effects are diminished.

In figs. 8, 9, and 10 we present the diagrams obtained with the Geiger-instruments (top) and those obtained with the Stoppani-instruments (bottom). It is apparent that both the general shape of the curves and the frequency of vibration as obtained with the two instruments are in good accordance. The magnitude of the amplitudes show, however, distinctly differing values. While the Geiger-instruments registered amplitudes of about 28% of the statical

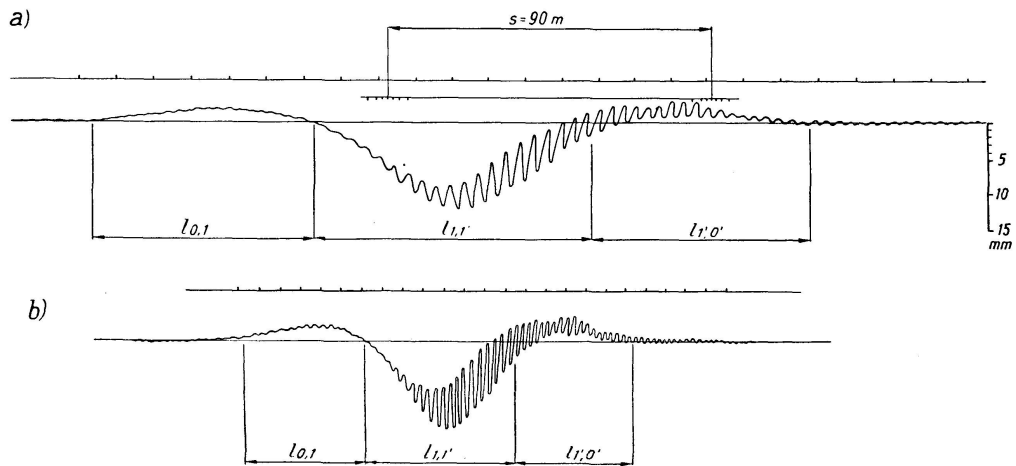


Fig. 8. Deflection of Centre of Middle-Span Recorded when the Locomotive is Driving at 37 km p. h. a) Geiger-Instrument; b) Stoppani-Instrument.

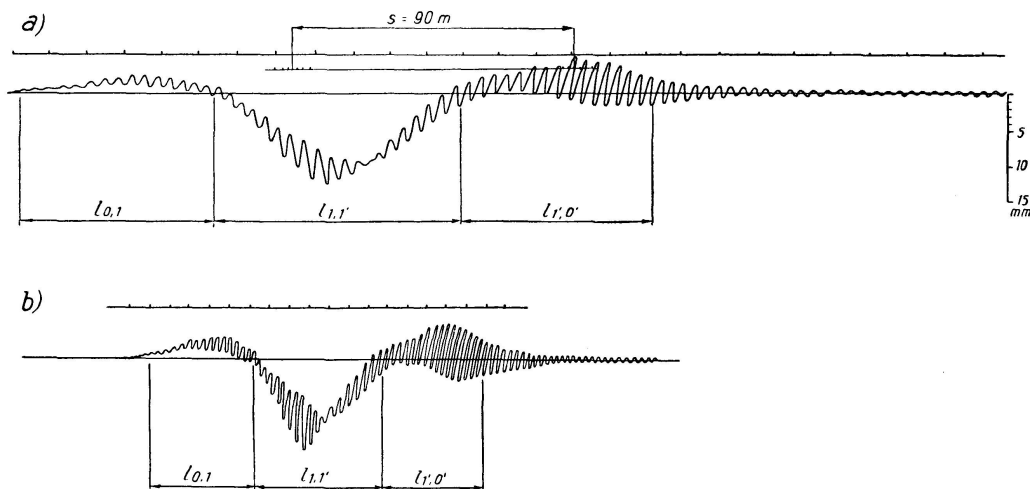


Fig. 9. Diagram Recorded at the Speed of Two-Cylinder Locomotive 42.5 km p. h. a) Geiger-Instrument; b) Stoppani-Instrument.

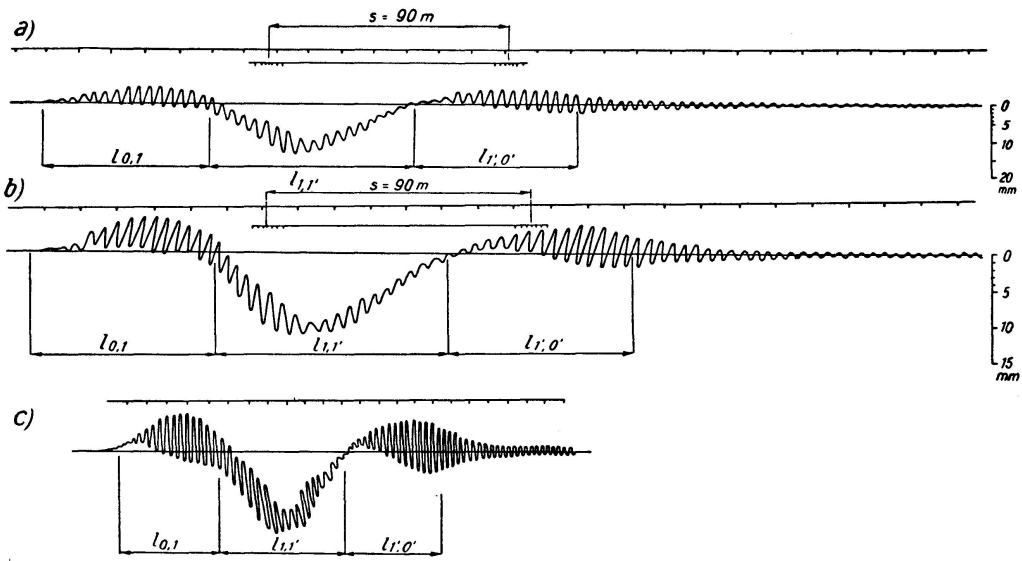


Fig. 10. Diagram Recorded at the Speed of Two-Cylinder Locomotive 44 km p. h.

- a) Geiger-Instrument on Cantilever;
- b) Geiger-Instrument with Wire-Connection to Fixed Point at River Bottom;
- c) Stoppani-Instrument.

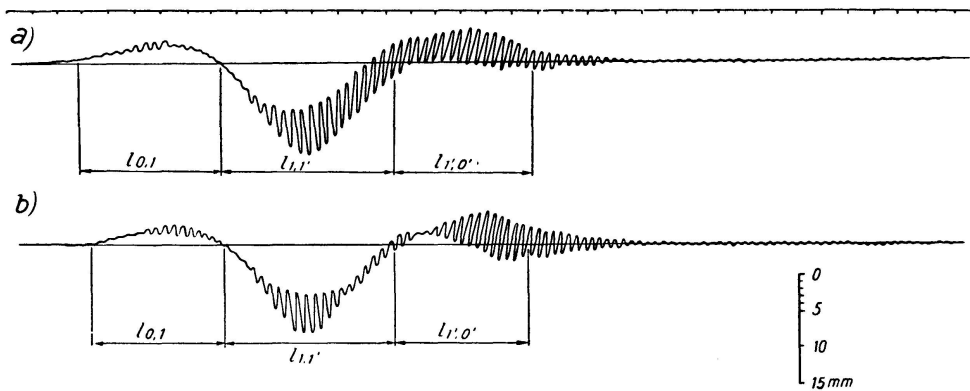


Fig. 11. Record of Geiger-Instrument at Centre of Middle-Span for Speed of Two-Cylinder Locomotive. a) Speed 40 km p. h. ; b) Speed 42 km p. h.

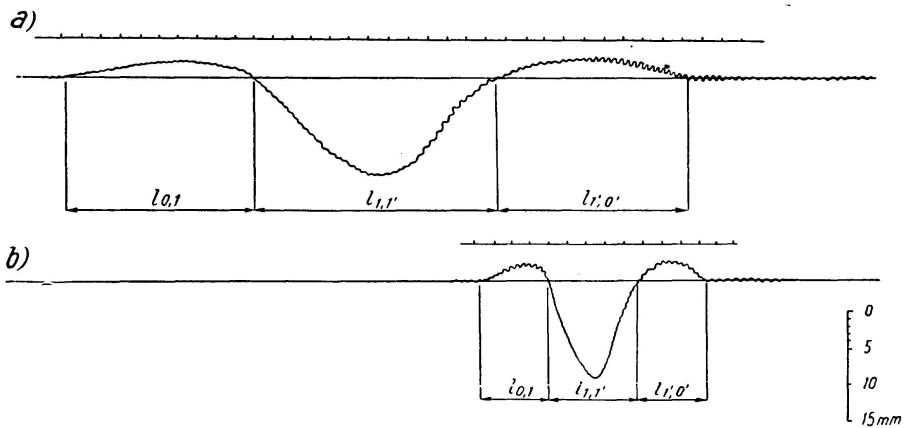


Fig. 12. Recorded Deflection at Centre of Middle Span, Three-Cylinder Locomotive Driving at a) Speed 22.5 km p. h. ; b) Speed 61 km p. h.

deflection, the Stoppani-instruments registered much larger values, viz. about 40% of the statical deflection. The author is of the opinion, that the registrations of the Geiger-instruments were distorted by the friction between the needle and registration paper, which resulted in diminishing the registered magnitudes of the amplitudes.

The Geiger- and Stoppani-instruments have been screwed onto the girders of the bridge and connected to a fix point at the bottom of the river by means of a 10-m long steel wire. The described arrangement has been much commented upon, the main objection being that the obtained results are affected by the vibration of the wire connection. Check-tests have therefore been carried out, having the registering Geiger-instrument fixed to a cantilever of the tested bridge, while the fixed point was situated on a cantilever of the adjoining bridge which carried the parallel second track. Each bridge having separated under-structure it could be assumed that the second-track bridge was practically at rest during the experiment. The results of these check-tests are given in fig. 10a. Fig. 10b shows the corresponding record of the second Geiger-instrument, which had the wire-connection mentioned above, and fig. 10c shows the record of the Stoppani deflection-meter. It is apparent, that the records of the two Geiger-instruments differ only very slightly (the second diagram is twice enlarged).

In fig. 12 the record is given, obtained while a three-cylinder express locomotive was crossing the bridge. No resonance vibration corresponding to the first natural frequency could be observed.

#### IV. Comparison of the Theoretical and Experimental Results

The theoretical analysis had to be considerably simplified and some factors could not be taken into account at all, so that we cannot expect the theoretical results to be in full accordance with results obtained experimentally. The theoretically obtained curves as shown in figs. 4c and 5 may, however, be regarded as well representing the nature of the vibration of continuous beams, if the structure is crossed by a two-cylinder locomotive. The differences between the theoretical and measured values show the extent to which the neglected factors affect the accuracy of the analysis.

The first factor which has been neglected in the above given solution is that the analysis had been carried out by expanding the vibration into the series of natural modes and considering only the first term of the series, i. e. *neglecting all higher modes*. It is obvious, that if we considered also the higher modes, we might obtain larger amplitudes. The author had pointed out the possibilities in this respect in his previous paper<sup>12)</sup>, where he gave the analysis

---

<sup>12)</sup> KOLOUŠEK, "Schwingungen der Brücken aus Stahl und Stahlbeton". Mémoires de l'AIPC T. XVI. Zurich 1956.

of an arch bridge continuous over 15 spans. In what follows we shall try to give a rough estimate of the influence of the higher modes. For that reason we shall compute the second and third natural frequencies and the corresponding natural modes.

The second natural mode is anti-symmetrical and for the second natural frequency the following equation has to hold true:

$$\frac{J_{0,1}}{l_{0,1}} F_7(\lambda_{0,1}) = \frac{J_{1,1'}}{l_{1,1'}} [-F_1(\lambda_{1,1'}) - F_2(\lambda_{1,1'})].$$

The equation holds true for

$$\lambda_{0,1} = 3,58, \quad \lambda_{1,1'} = 4,12,$$

so that the second natural frequency is

$$n_{(2)} = 4,89 \text{ s}^{-1}.$$

The constants of integration in eq. (4) are determined similarly as for the first natural mode. Assuming  $\gamma_1 = \gamma_{1'} = 1$  we obtain for the end span

$$v_{(2)}(x) = -0,835 \sinh 3,58 \frac{x}{l} - 35,4 \sin 3,58 \frac{x}{l}$$

and for the second span

$$v_{(2)}(x) = -12,0 \cosh 4,12 \frac{x}{l} + 12,4 \sinh 4,12 \frac{x}{l} + 12,0 \cos 4,12 \frac{x}{l} + 6,4 \sin 4,12 \frac{x}{l}.$$

The second natural mode is shown in fig. 3 b.

The third natural mode is again symmetrical, and the third natural frequency is given by eq. (36). We obtain

$$\lambda_{0,1} = 3,99, \quad \lambda_{1,1'} = 4,59, \\ n_{(3)} = 6,08 \text{ s}^{-1}.$$

For the span 0,1 we have

$$v_{(3)}(x) = 4,82 \sinh 3,99 \frac{x}{l} + 17,47 \sin 3,99 \frac{x}{l}$$

and for the span 1,1'

$$v_{(3)}(x) = 112,5 \cosh 4,59 \frac{x}{l} - 110,2 \sinh 4,59 \frac{x}{l} - 112,5 \cos 4,59 \frac{x}{l} + \\ + 127,1 \sin 4,59 \frac{x}{l}.$$

The third natural mode is shown in fig. 3 c.

It is obvious, that the second natural mode does not affect (because of its anti-symmetry) the deflection of the point "s". The third natural frequency reaching almost twice the value of the first one, the neglect of the third

mode seems for the first critical speed to be fully entitled. In practical cases, however, we cannot exclude the possibility of the second or even the third critical speed to be attained.

We have already mentioned *the second inaccuracy* introduced into the theoretical analysis by *neglecting the movement of the inertial mass* along the structure. If the mass of the locomotive is presumed to be steadily placed at the centre of the middle span, we obtain a lower natural frequency than if the mass be placed in the first span. This fact is obvious also from fig. 8, where we present the record obtained with deflection meters applied for the locomotive driving at 37 km p. h. The diagram shows, that maximum vibration effects take place when the engine is crossing the middle span. The experimentally obtained curve of fig. 8 is similar to the theoretical curve of fig. 5. If the speed is higher, vibration of the whole structure is excited by the engine crossing any of the spans. For still higher speeds the vibration of the bridge is excited mainly when the engine is crossing the end spans. This is apparent also from fig. 10, where the respective speed is 44 km p. h.

The variability of the natural frequency results in diminishing the amplitudes and so it has a similar effect as damping. Thus better accuracy of the analysis is obtained if we assume a higher damping factor for the calculations.

### Summary

This paper gives theoretical and experimental analysis of the dynamical effects of a two-cylinder locomotive with unbalanced driving axles crossing a bridge continuous over three spans.

The theoretical analysis has been carried out by expanding the vibrations into the series of natural modes. The actual structure has been for analytical purposes replaced by a substitute three-span truss, with cross-section constant within the individual spans. The natural frequencies and modes may thus be analysed with the aid of the tables of  $F(\lambda)$ -functions<sup>13</sup>). The movement of the inertial mass of the engine along the bridge has been neglected, as the mass is small in comparison to the mass of the bridge.

The theoretical analysis is, because of these assumptions, not exact, but a comparison of the theoretical and experimentally obtained results shows, that the presented analysis approximates the actual dynamical behaviour of the structure with sufficient accuracy for practical purposes.

### Résumé

L'auteur étudie théoriquement et expérimentalement les influences dynamiques qui se manifestent au cours du passage d'une locomotive à deux

---

<sup>13</sup>) See e. g. ref. 1).

cylindres, à essieux moteurs non équilibrés, sur un pont à poutres continues à trois travées.

L'étude théorique a été effectuée par développement des vibrations en séries de vibrations propres. Pour simplifier le calcul, le système porteur effectif a été remplacé par une poutre en treillis à trois travées avec section constante dans chaque travée. Les fréquences et vibrations propres peuvent ainsi être étudiées à l'aide des tableaux relatifs aux fonctions  $F(\lambda)$ . Le mouvement de la masse d'inertie de la locomotive sur le pont a été négligé, car cette masse est faible par rapport à celle du pont.

Sur la base des hypothèses ci-dessus, l'étude théorique n'est pas rigoureusement exacte; néanmoins, la comparaison entre les résultats théoriques et les résultats expérimentaux montre que cette méthode d'investigation du comportement dynamique de la construction fournit une approximation suffisante pour les besoins de la pratique.

### Zusammenfassung

Dieser Aufsatz beschreibt die theoretische und experimentelle Untersuchung der dynamischen Wirkungen bei der Fahrt einer Zweizylinder-Lokomotive mit nicht ausgewuchteten Triebachsen über eine dreifeldrige Durchlaufträgerbrücke.

Die theoretische Untersuchung wurde ausgeführt durch Entwicklung der Schwingungen in Reihen nach Eigenschwingungsformen. Das effektive Tragwerk wurde zur Rechnungsvereinfachung durch einen dreifeldrigen Träger mit feldweise konstantem Querschnitt ersetzt. Die Eigenfrequenzen und -schwingungen können so mit Hilfe der Tabellen für  $F(\lambda)$ -Funktionen untersucht werden. Die Bewegung der Trägheitsmasse der Lokomotive über die Brücke wurde vernachlässigt, da diese Masse klein ist im Vergleich mit derjenigen der Brücke.

Auf Grund dieser Annahmen ist die theoretische Untersuchung nicht genau, aber der Vergleich von theoretisch und versuchstechnisch erhaltenen Resultaten zeigt, daß die dargelegte Untersuchung eine für praktische Zwecke genügende Näherung an das effektive, dynamische Verhalten des Tragwerks gibt.